Supporting Information

One-dimensional Confined p–n Junctions Co_3S_4/MoS_2 Interface Nanorod Significantly Enhancing Polysulfides Redox Kinetics for Li-S Battery

Wei Zhou [a,b,#], *Shunlian Ning* [c,#], *Bin Fan* [b,#], *Qikai Wu* [b], *Luo Mi* [b], *Dengke Zhao* [d,*], *Kai Zhou* [e,*], *and Nan Wang* [a,*]

a. Siyuan laboratory, Guangzhou Key Laboratory of Vacuum Coating Technologies and New Energy Materials, Department of Physics, Jinan University, Guangzhou, Guangdong 510632, China.

b. New Energy Research Institute, College of Environment and Energy, South China University of Technology, Guangzhou 510006, China.

c. School of Chemistry, Sun Yat-sen University, Guangzhou, Guangdong 510275, China.

d. School of Materials Science and Engineering, Henan Normal University, Xinxiang 453007, China.

e. Guangzhou Key Laboratory of Sensing Materials and Devices, Center for Advanced Analytical Science, c/o School of Chemistry and Chemical Engineering, Guangzhou University, Guangzhou 510006, P.R. China.

Email: scutezhao@sina.com (Dekeng Zhao); cckzhou@gzhu.edu.cn (K. Zhou); nanwang@email.jnu.edu.cn (*N. Wang).*

* The corresponding author

# These authors contributed equally to this work.

Experimental Section

Preparation of MoO_3 nanorod (MoO_3 NR): In simple, 1.4 g ammonium molybdate was dispersed into 25 mL distilled water (DI) and 5 mL HNO_3 (68 wt.%) mixture and sonicated for 30 min. Next, the mixture was taken placed into Teflon autoclave and hydrothermal treatment at 200 ℃ for 20 h. After cooling to room temperature, the MoO_3 NR was acquired via centrifugation and drying at 60 °C for 12 h.

Preparation of MoO_3@ZIF-67 NR and ZIF-67: In short, 200 mg as-fabricated MoO_3 NR was dissolved into 100 mL DI and ultrasound for 30 min. Next, 1.46 g Co $(NO_3)_2 \cdot 6H_2O$ was added to the mixture and followed by stirring for 30 min to form A solution. Then, 3.28 g 2-dimethylimidazole (0.04 M) aqueous solution was slowly dripped into A solution with vigorous stirring and stand for 24 h. After that, the MoO_3@ZIF-67 precursor was formed via filtration, washed with DI, and dried at 60 °C for 12 h. The preparation procedure of ZIF-67 is consistent with that of MoO_3@ZIF-67 NR, except for eliminating the MoO_3 NR.

Preparation of n-Co_3S_4/p-MoS_2 NR, MoS_2 NR, Co_3S_4 and MoS_2: 50 mg MoO_3@ZIF-67 precursor was dissolved into 10 ml ethylene glycol (EG) and ultrasound for 30 min. Next, 200 mg thiourea was also dispersed into the above mixture and ultrasound for10 min. Subsequently, 5 ml hydrazine hydrate was dripped into the above mixture and stirred for 5 min. Next, the mixture was taken placed into Teflon autoclave and hydrothermal treatment at 200 ℃ for 24 h. The n-Co_3S_4/p-MoS_2 NR materials were obtained via filtration and vacuum drying overnight. p-MoS_2 NR and n-Co_3S_4 were synthesized in the same way employing MoO_3 NR and ZIF-67 as the precursor, respectively.

For comparison, the MoS_2 samples were obtained by one-step hydrothermal reaction of

ammonium molybdate and thiourea.

Preparation of S@n-Co_3S_4/p-MoS_2 NR: The n-Co_3S_4/p-MoS_2 NR and sulfur (weight ratio: 1:4) were uniformly ground in mortar and then placed to a quartz tube. Then, the mixture was first heated at 155 °C for 12.0 h and further annealed at 200 ℃ for 1 h under an Ar atmosphere. After returning to room temperature, the S@n-Co_3S_4/p-MoS_2 NR was formed.

Electrochemical measurements

The S@n-Co_3S_4/p-MoS_2 NR, acetylene black, and Polyvinylidene fluoride (PVDF) with the weight ratio of 7:2:1 is uniformly mixed in N-methyl-2-pyrrolidene (NMP) and followed via stirring at room temperature for 7.0 h to obtain the uniform slurry. Then, the as-prepared slurry was coated on aluminum foil and subsequently dried at oven for 12 h. The various areal sulfur loading cathode were obtained by changing the thickness of slurry casting. The assembled CR2032-type coin cells employed the S@n-Co_3S_4/p-MoS_2 NR composites as the cathode, Li foil as the anode, Celgard 2400 as the separator, and 1 M of lithium bis (trifluoromethanesulfonyl)imide (LiTFSL) in DOL/DME solvent (V_{DOL} /V_{DME}=1:1) with 2% $LiNO_3$ as the electrolyte. The ratio of the electrolyte and sulfur (E/S) was demanded at 15 μL mg^{-1} for regular batteries. In view of high-loading cathodes, the E/S ratio was 7 - 5 μL mg^{-1}. The electrochemical impedance spectroscopy (EIS) and cyclic voltammetry (CV) experiments were recorded by the CHI660E workstation. Galvanostatic intermittent titration (GITT) tests were conducted via a current pulse at 0.20 mA for 10 min and then with 0.5 h of rest.

Lithium polysulfides (LiPSs) adsorption experiment: Li_2S_6 solution (0.1M) was obtained via dissolving the sulfur and Li_2S (the molar ratio: 5:1) in tetrahydrofuran (THF) solution. Next, the different powders with same weight were added into 5 mL of Li_2S_6

solution for standing 1h, respectively. The adsorption performances of different as-synthesized samples towards Li_2S_6 were conducted by the UV-vis spectra.

Symmetric cell experiment: The as-fabricated materials, Super P, and PVDF with the weight of 7:2:1 was dissolved into NMP and coated on the carbon cloth to form the working and counter electrodes. The electrolyte is obtained via mixing the 0.2 M Li_2S_6 into regular electrolyte. To estimate the electrochemical properties, the CHI660E workstation was employed to test the CV and EIS measurements.

Li_2S nucleation experiment: The 1D n-Co_3S_4/p-MoS_2 NR, p-MoS_2 NR or MoS_2 was coated on carbon cloth as the cathode, and Li foil was employed as the anode for the testing. The electrolyte was 0.2 M Li_2S_8 dispersed in tetraglyme solvent. The cells were first discharged at 0.112 mA to 2.06V and followed were potentiostatically discharged at 2.05V until the current was below 10^{-5} mA.

Materials characterization

The scanning electron microscope (S-4800, Hitachi) and a transmission electron microscope (TEM, JEOL JEM-2100) were performed to inspect the morphologies of as-obtained materials. X-ray diffraction (XRD, Bruker D8-Advance) was conducted to estimate the crystalline structure of as-prepared materials. Thermogravimetric analysis (TGA) of sulfur composites was evaluated by TGA-METTLER in N_2. The specific surface area and pore size distribution of the all samples were acquired via the Nitrogen adsorption−desorption measurement. The XPS spectrum was carried out by Casa XPS software. The laser Raman spectrometer was used to investigate the Raman spectra. The UV2600 was performed to evaluate the LiPSs adsorption performance.

Density functional theory (DFT)

DFT calculations were performed with the open-source planewave code, Quantum Espresso. In all calculations, the spin polarized generalized gradient approximation (GGA) of the Perdew–Burke–Ernzerhof (PBE) functional and ultrasoft pseudo-potentials were used for the core electrons. The plane-wave cutoff energy was set to ‘‘fine”. The convergence of forces and energy on each atom during structure relaxation were set to 0.04 eV $Å^{-1}$ in force and 10^{-6} eV in energy, respectively. The Brillouin zone was sampled with a 3 × 3 × 1 Monkhorst-Pack k-point grid. The vacuum space along the z-direction was more than 15 Å, large enough to avoid interplanar interactions. For geometry optimization of all slab models, the top two layers were allowed to relax. The adsorption energies (E_a) for Li_2S_6 on the surfaces are defined as $E_a=E_{total}–E_{ads}–E_{slab}$, where E_{total} is the total energy of the adsorbed system, E_{ads} is the energy of the adsorbate Li_2S_6 in vacuum and E_{slab} is the energy of the optimized clean surface slab.

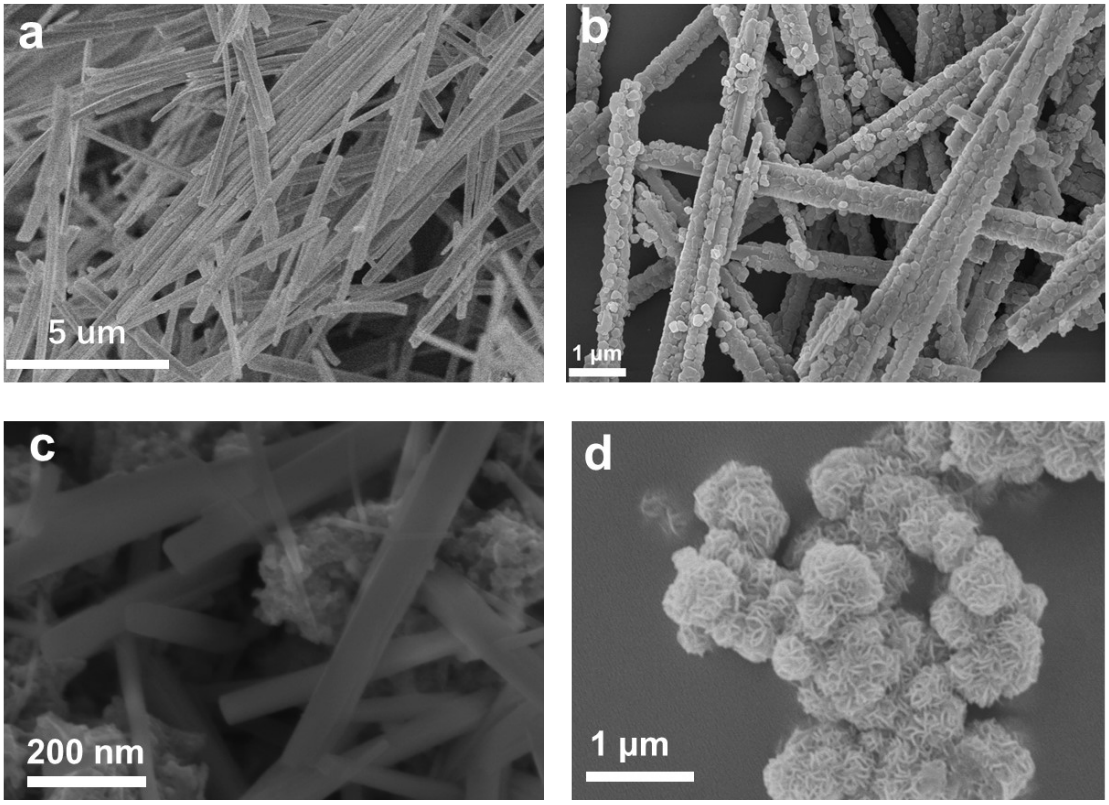

Figure S1. SEM images of (a) MoO_3 NWs. (b) MoO_3@ZIF. (c) MoS_2 NR. (d) MoS_2.

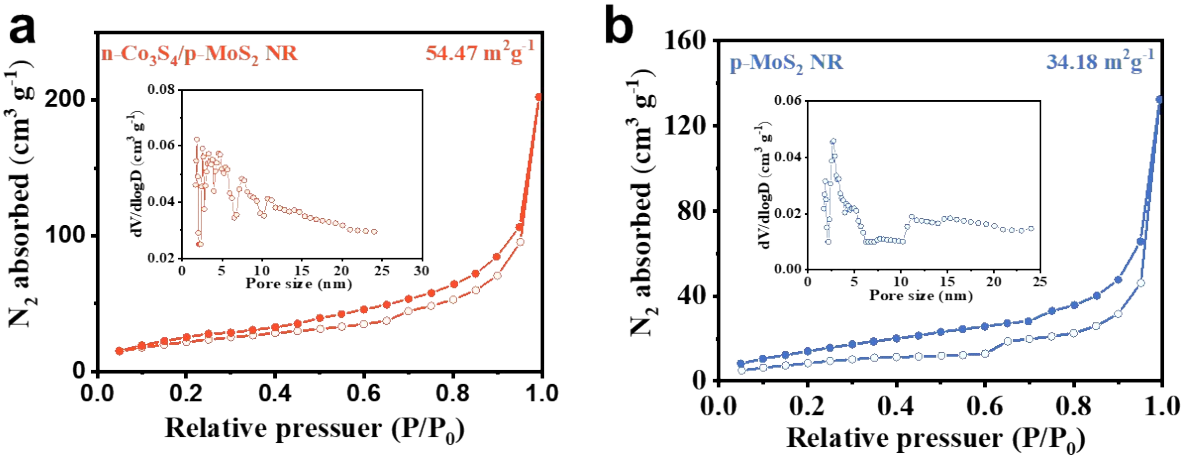

Figure S2. Nitrogen adsorption/desorption isotherms of (a) M/S-Co_3S_4/MoS_2 NR and (b) MoS_2 NR, where the inserts are the relevant pore size distribution.

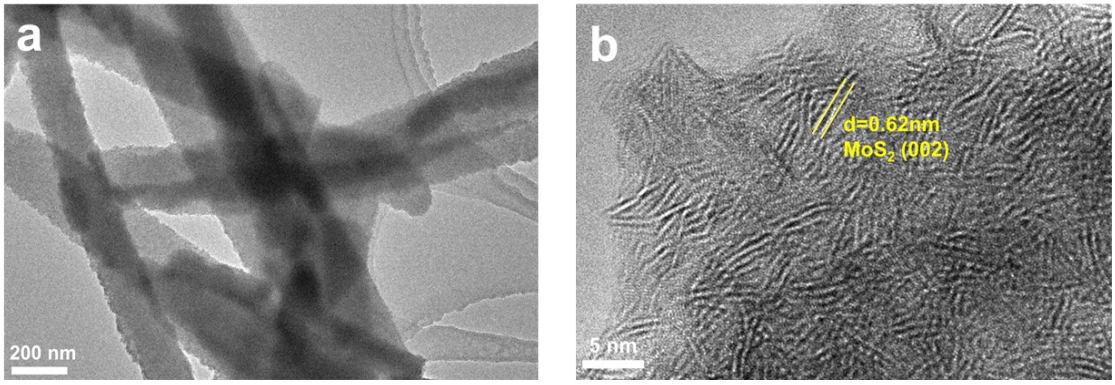

Figure S3. (a, b) The TEM and HRTEM images of HRTEM of MoS_2 NR.

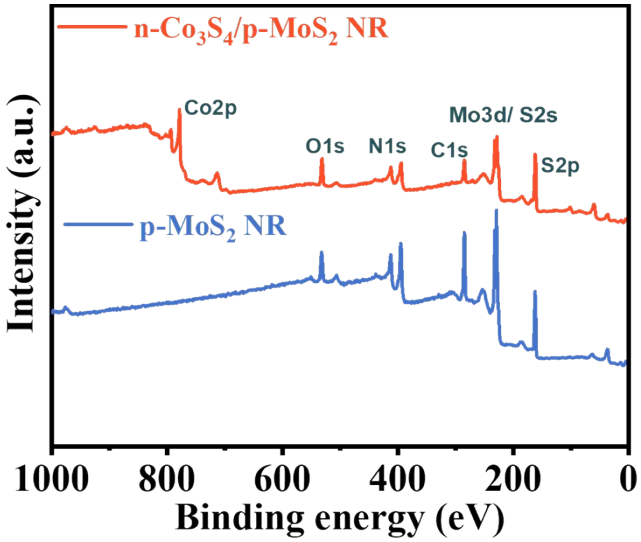

Figure S4. XPS survey scan of n-Co_3S_4/p-MoS_2 NR and MoS_2 NR.

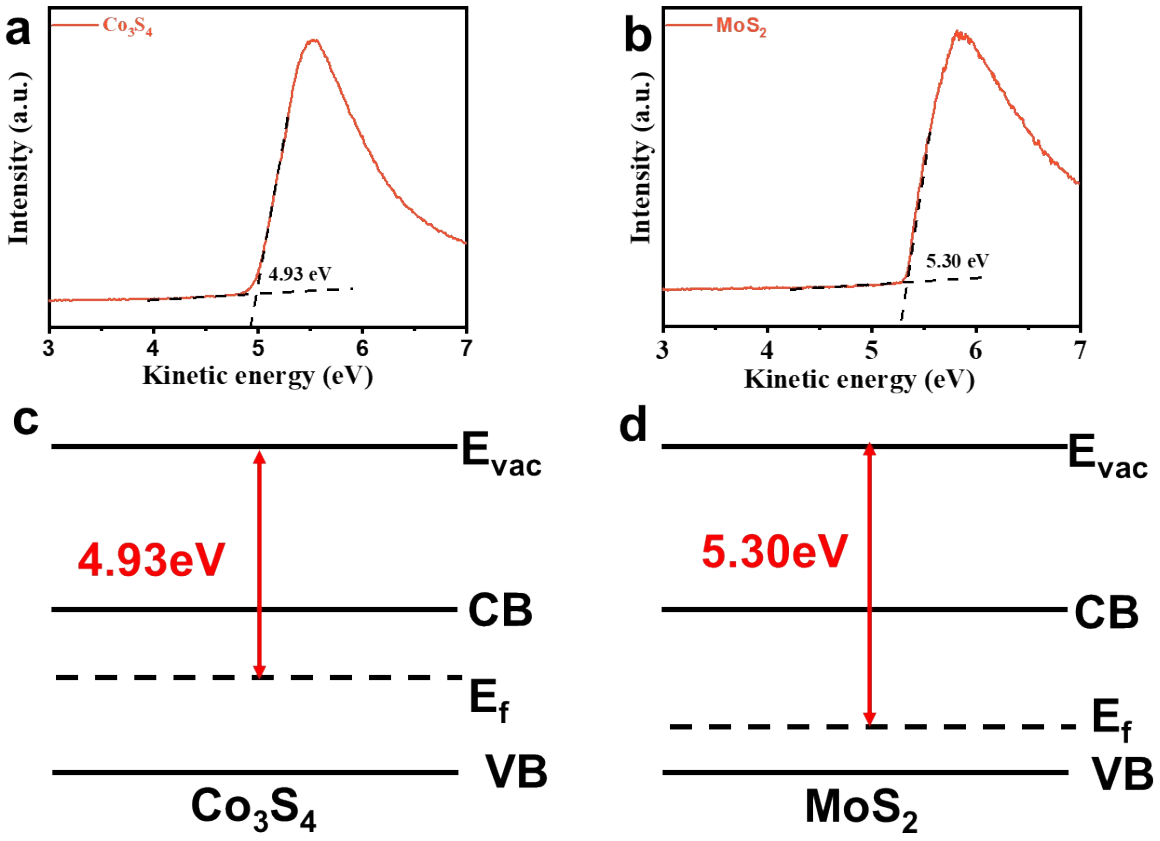

Figure S5. XPS valence band spectra and the work function Φ. (a, c) Co_3S_4 and (b, d) MoS_2.

The work function (Φ) of Co_3S_4 and MoS_2 materials are calculated via the equation of $\Phi = h\upsilon - (E_{Fermi,\ K} - E_{SE\ Cuttof,\ K})$, where the $E_{Fermi,\ K}$ is 1486.6 eV and monochromatic Photon Energy ($h\upsilon$) for XPS is 1486.6 eV. Therefore, $\Phi = E_{SE\ Cuttof,\ K}$ are as 4.93 and 5.30 eV , respectively.

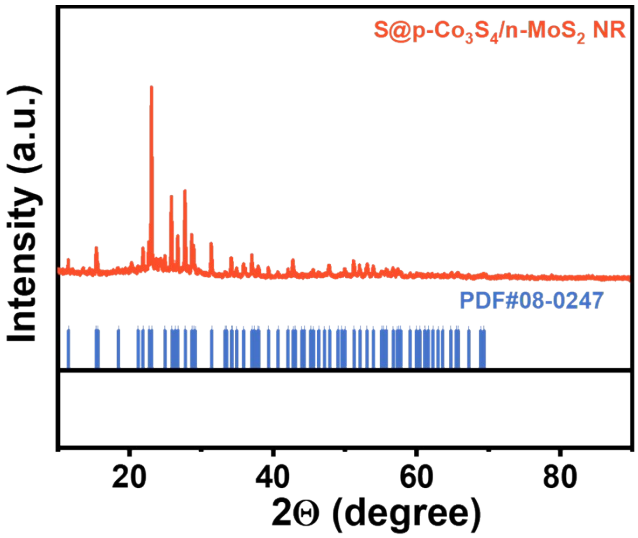

Figure S6. The XRD pattern of S@n-Co_3S_4/p-MoS_2 NR.

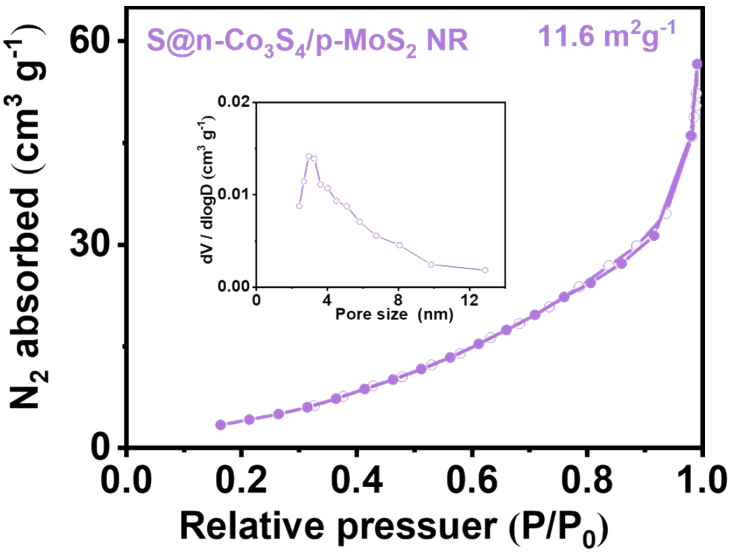

Figure S7. Nitrogen adsorption/desorption isotherms of S@n-Co_3S_4/p-MoS_2 NR, where the inserts are the relevant pore size distribution.

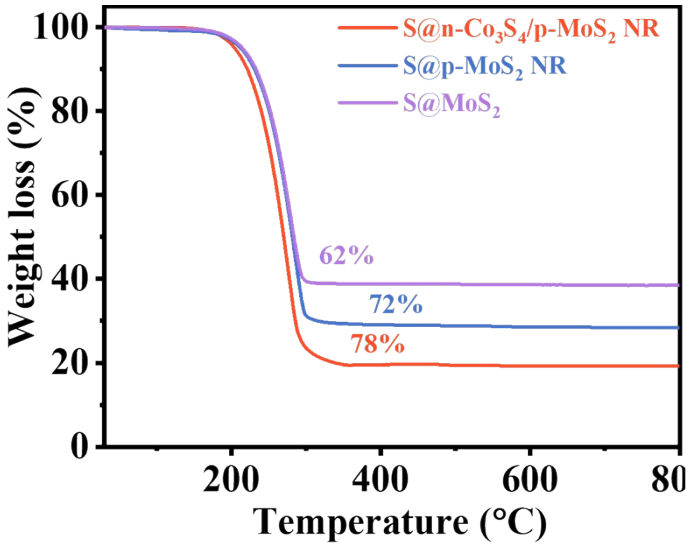

Figure S8. TGA profiles of S@n-Co_3S_4/p-MoS_2 NR, and S@p-MoS_2 NR, and S@ MoS_2.

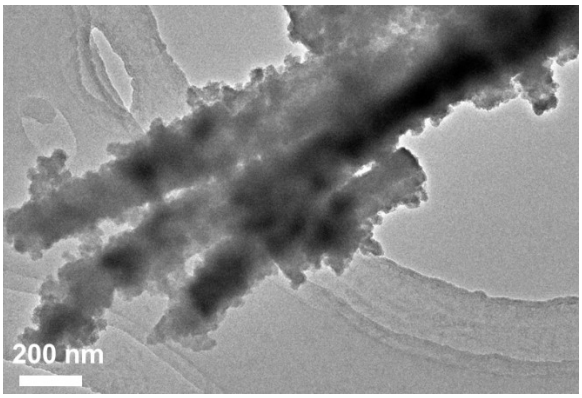

Figure S9. TEM image of S@n-Co_3S_4/p-MoS_2 NR composites.

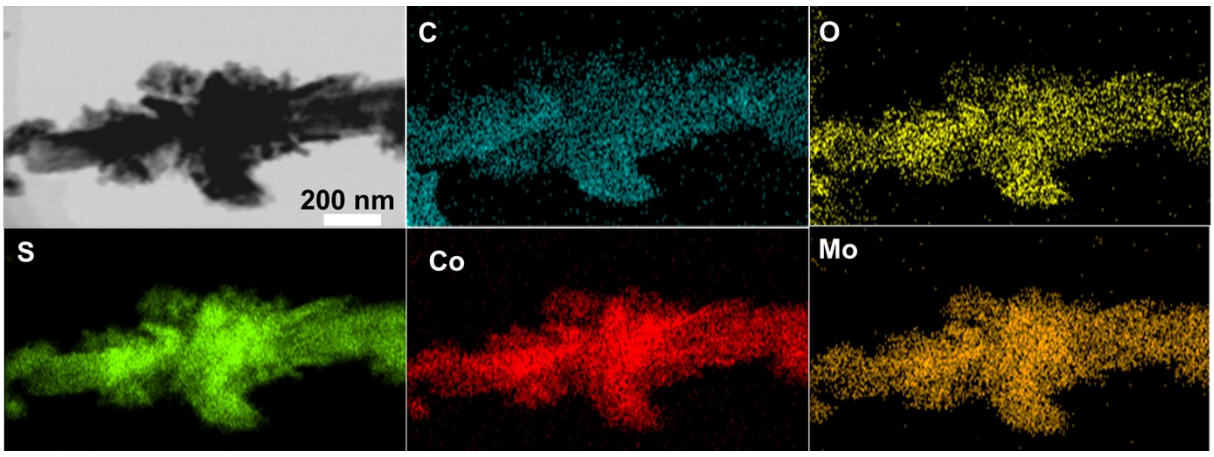

Figure S10. Elemental mapping images of S@n-Co_3S_4/p-MoS_2 NR composites.

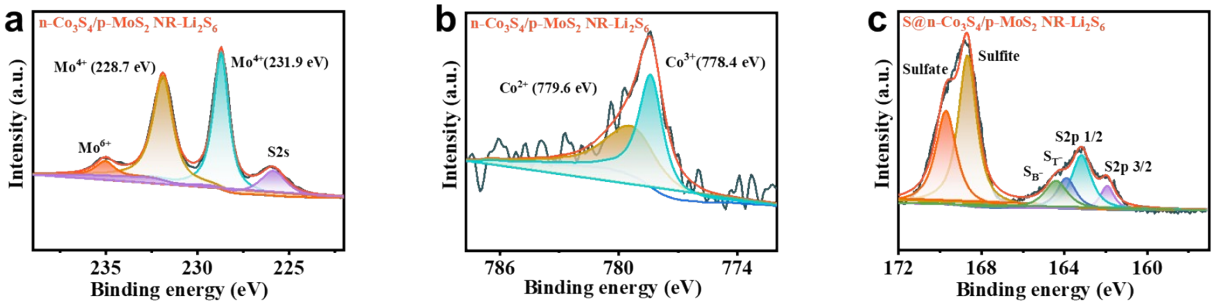

Figure S11. High-resolution XPS spectra of (d) S2p, (e) Mo3d, and (f) n-Co_3S_4/p-MoS_2 NR-Li_2S_6.

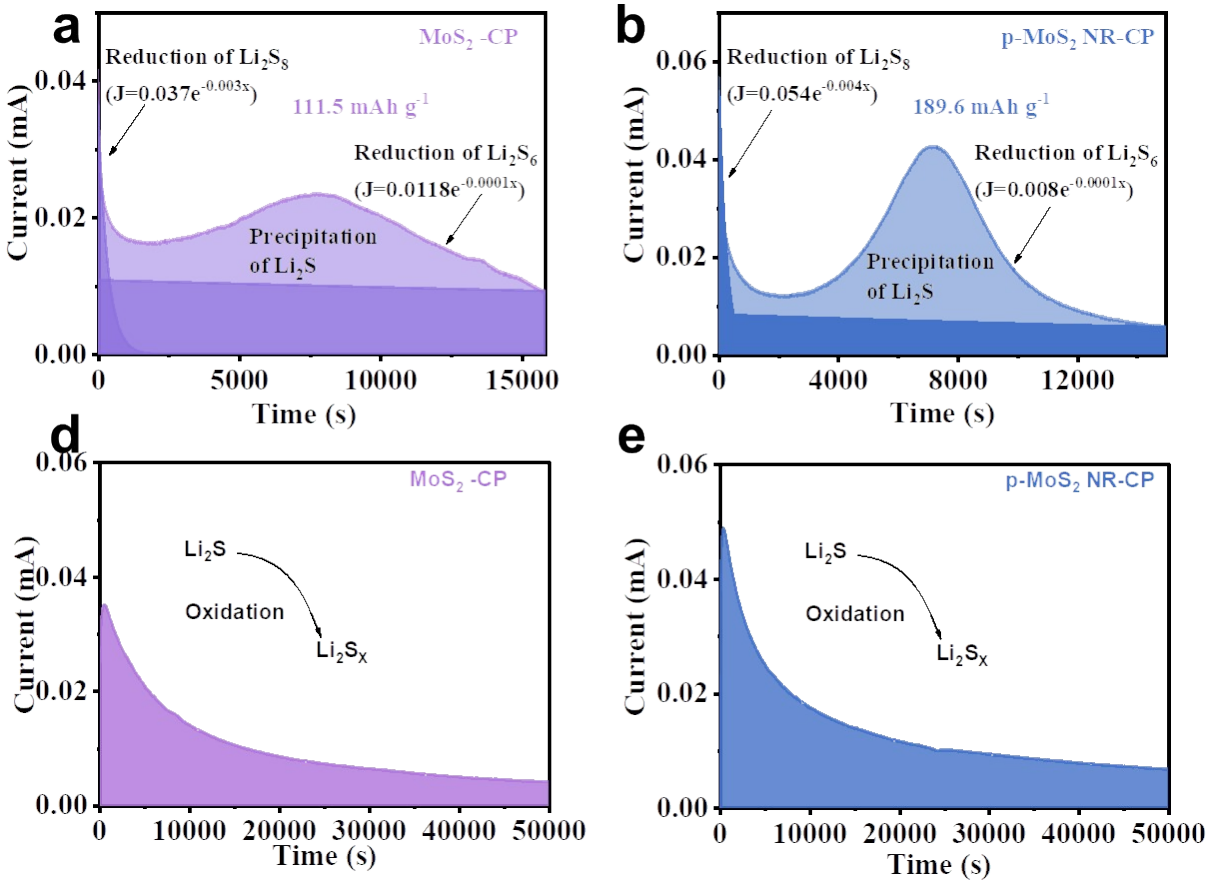

Figure S12. Potentiostatic discharge profiles of Li_2S_8 electrolyte at 2.05 V on (a)p-MoS_2 NR-CP, and (b) MoS_2-CP surface. (c-d) The dissolution profiles of Li_2S.

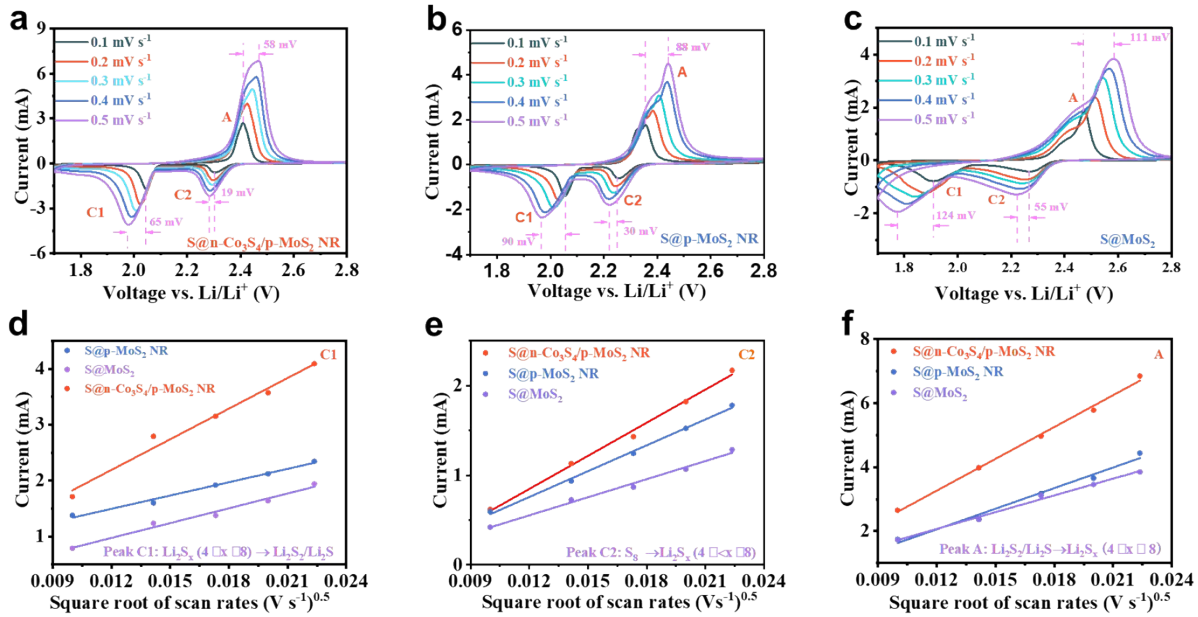

Figure S13. (a-c) CV curves of S@n-Co_3S_4/p-MoS_2 NR, S@p-MoS_2 NR and S@MoS_2 cathodes at scan rates 0.1- 0.5 mV s^{-1}. Current values of (c-d) the cathodic peaks and (e) the anodic peaks.

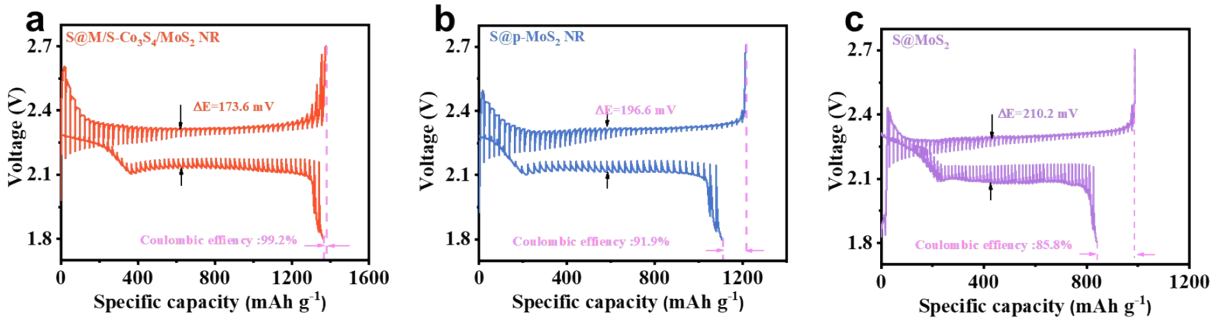

Figure S14. GITT profile of (a) S@n-Co_3S_4/p-MoS_2 NR, (b) S@p-MoS_2 NR and (c) S@MoS_2 cathodes.

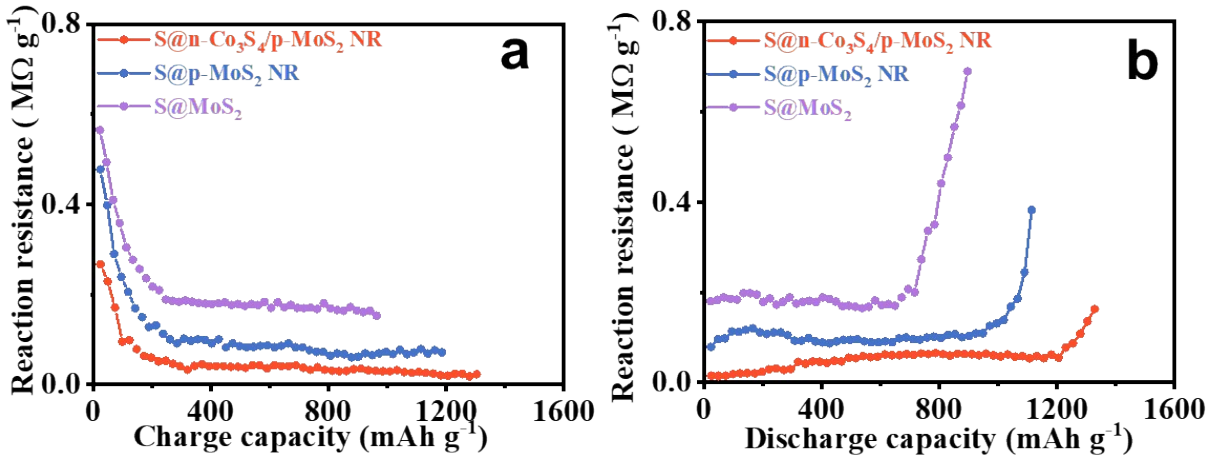

Figure S15. Reaction resistance of the three cathodes during the (e) charge and (f) discharge processes.

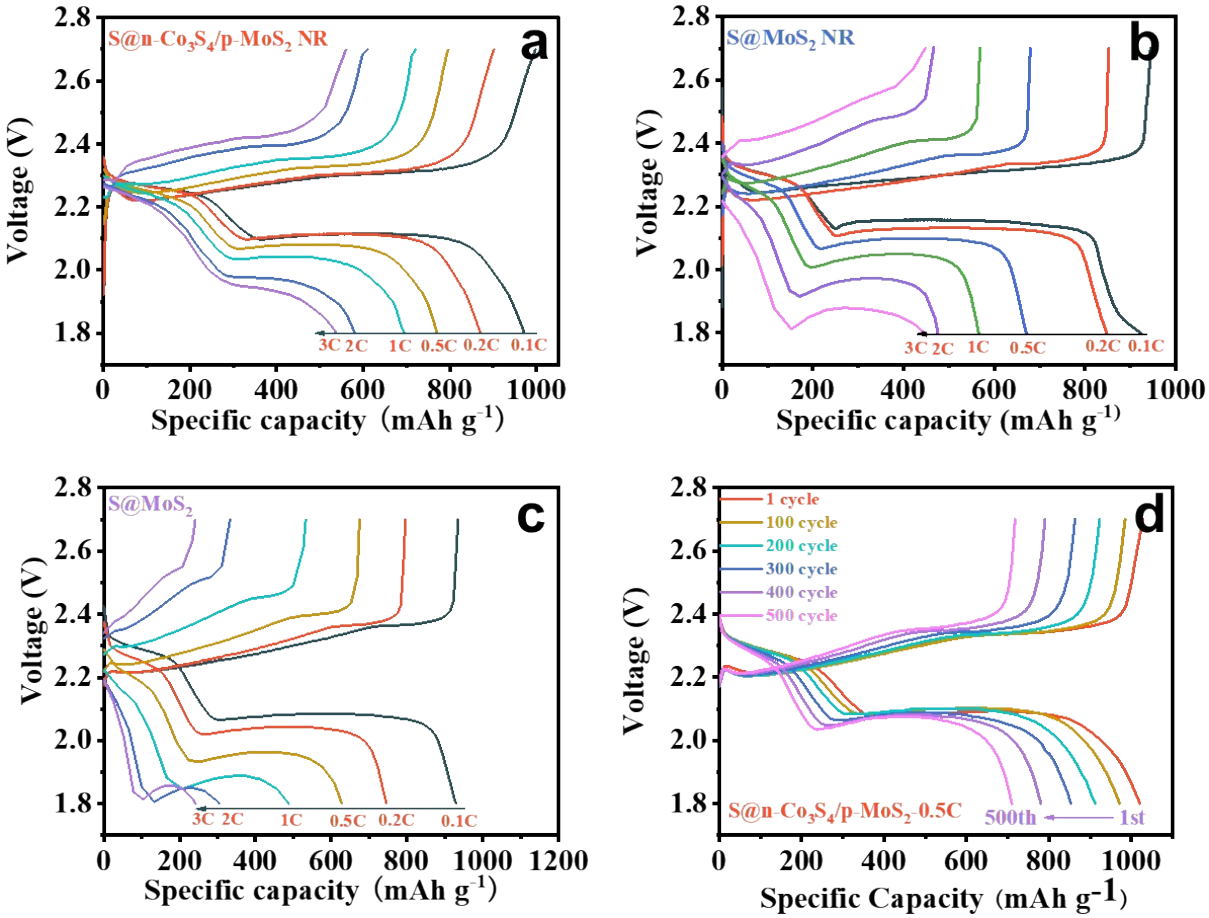

Figure S16. GCD profiles of (a) S@n-Co_3S_4/p-MoS_2 NR, (b) S@p-MoS_2 NR, and (c) S@MoS_2 cathodes at different current rates. (d) GCD profiles of S@n-Co_3S_4/p-MoS_2 NR cathode at 0.5C under different cycles.

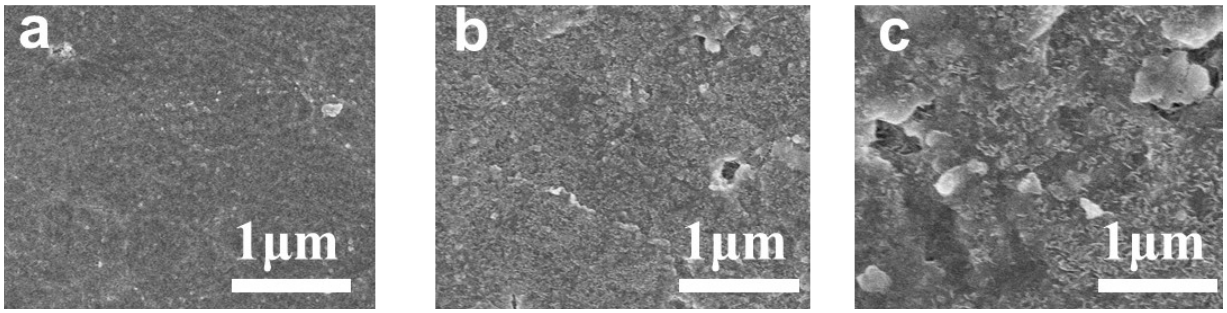

Figure S17. SEM images of the Li anode of (a) S@n-Co_3S_4/p-MoS_2 NR, (b) S@p-MoS_2 NR, and (c) S@MoS_2 cathodes after 500 cycles at 0.5C.

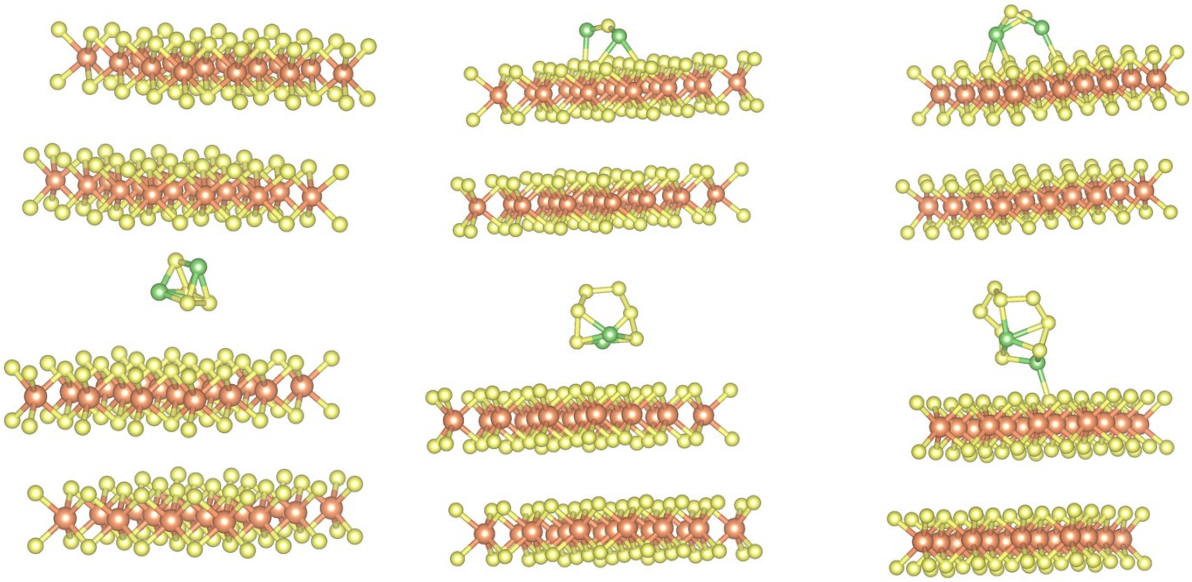

Figure S18. The optimal adsorption configuration of Li_2S_x (x=1, 2, 4, 6, 8) on MoS_2.

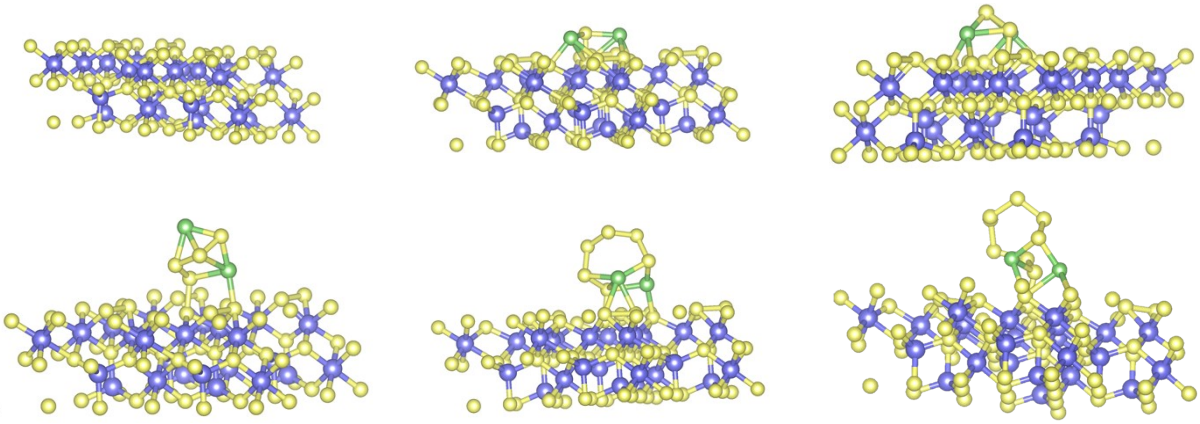

Figure S19. The optimal adsorption configuration of Li_2S_x (x=1, 2, 4, 6, 8) on Co_3S_4.

Equation S1:

$$t_{Li+} = \frac{I_{ss}(\Delta V - I_0 R_0)}{I_0(\Delta V - I_{ss} R_{ss})}$$

I_0 and I_{ss} represent the initial and steady state currents during a potentiostatic polarization procedure, respectively. R_0 and R_{ss} are defined as the initial and steady-state resistances, respectively. ΔV is shown to be the constant voltage (10 mV) and t_{Li+} means the lithium-ion transference number.

Equation S2:

Lithium-ion diffusion coefficient D_{Li+}(cm^2 s^{-1}) is estimated via the Randles-Sevick equation:

$I_p=2.69\times10^5 n^{1.5} S D_{Li+}^{0.5} C_{Li+} \upsilon^{0.5}$

where I_p represent the peak current, n is the number of electron transfer (n=2), S exhibits the electrode area, C_{Li+} indicates the lithium-ion concentration in the electrolyte, and υ is the scanning rate (V s^{-1}).

Table S1. The surface area, pore volume, and pore size of as-prepared materials.

Sample	***Surface area*** ***(m^2 g^{-1}))***	***pore volume*** ***(cm^3 g^{-1})***	***Pore size (nm)***
n-Co_3S_4/p-MoS_2 NR	54.47	*1.05*	*1.385*
p-MoS_2 NR	*34.18*	*0.79*	*0.923*
S@n-Co_3S_4/p-MoS_2 NR	*11.6*	*0.085*	*0.362*

Table S2. Discharge capacity of two cathodes during the firat 0.1 C and the values of Q1, Q2, and Q2/Q1.

Interlayer	*Q1(mAh g^{-1})*	*Q2(mAh g^{-1})*	*Q2/Q1*
S@n-Co_3S_4/p-MoS_2 NR	373.5	*765.6*	*2.05*
S@p-MoS_2 NR	*351.9*	*672.2*	*1.91*
S@MoS_2	*294.9*	*542.8*	*1.84*

Table S3. Comparison of electrochemical performance of S@Co_3S_4/MoS_2 NR cell with other sulfur cathodes.

Sulfur host	*Sulfur loading (mg cm^{-2})*	*Current rate (C)*	*Capacity (mAh·g^{-1})*	*Areal capacity (mAh·cm^{-2})*	*E/S (μL g^{-1})*	*Ref.*
N-RGO@MoS_2	1.5-2.0	0.3	709.4			S1[1]
MHCS@MoS_2	1.5	1.0	735.7			*S2*[2]
MoS_2 –MoN	1.2	2.0	459	10.3	*6.3*	*S3*[3]
MoS_2/S/rGO	0.9-1.0	2.0	750			S4[4]
Mxene/1T-2H MoS_2 –C	1.0	0.5	799	*3.6*	*8.7*	S5[5]
GA/MoS_2	1.5	2.0	600			S6[6]
NC@MoS_2	1.5	2.0	600	3.26	20	S7[7]
Edg-MoS_2/CHMs	1.7	1.0	494	6.1	8.3	S8[8]
n--Co_3S_4/p-MoS_2 NR	**2.0**	**2.0**	**661.4**	**14.82**	**5**	**This work**

References:

1. Z. Li, S. Deng, R. Xu, L. Wei, X. Su and M. Wu, *Electrochimica Acta*, 2017, **252**, 200-207，DOI: 10.1016/j.electacta.2017.09.001.
2. Q. Shao, P. Lu, L. Xu, D. Guo, J. Gao, Z.-S. Wu and J. Chen, *Journal of Energy Chemistry*, 2020, **51**, 262-271, DOI: 10.1016/j.jechem.2020.03.035.
3. S. Wang, S. Feng, J. Liang, Q. Su, F. Zhao, H. Song, M. Zheng, Q. Sun, Z. Song, X. Jia, J. Yang, Y. Li, J. Liao, R. Li and X. Sun, Adv. Energy Mate, 2021, 11. 2003314, DOI: 10.1002/aenm.202003314.
4. Y. Wei, Z. Kong, Y. Pan, Y. Cao, D. Long, J. Wang, W. Qiao and L. Ling, *Journal of Materials Chemistry A*, 2018, **6**, 5899-5909, DOI: 10.1039/c8ta00222c.
5. Y. Zhang, Z. Mu, C. Yang, Z. Xu, S. Zhang, X. Zhang, Y. Li, J. Lai, Z. Sun, Y. Yang, Y. Chao, C. Li, X. Ge, W. Yang and S. Guo, *Advanced Functional Materials*, 2018, **28**, DOI: 10.1016/j.cej.2020.128102.
6. M. Liu, C. Zhang, J. Su, X. Chen, T. Ma, T. Huang and A. Yu, *ACS Appl Mater Interfaces*, 2019, **11**, 20788-20795, DOI: 10.1021/acsami.9b03011.
7. W. Yang, W. Yang, L. Dong, X. Gao, G. Wang and G. Shao, *Journal of Materials Chemistry A*, 2019, **7**, 13103-13112, DOI: 10.1039/c9ta03227d.
8. N. Zheng, G. Jiang, X. Chen, J. Mao, N. Jiang and Y. Li, *Nanomicro Lett*, 2019, **11**, 43, DOI: 10.1007/s40820-019-0275-z.